Proceedings of the 45th IEEE Conference on Decision & Control
Manchester Grand Hyatt Hotel
San Diego, CA, USA, December 13-15, 2006

Optimal Digitizing Method with Application to the Design of Digital Control Systems

Grigore I. Braileanu, *Senior Member, IEEE*

***Abstract* – In digital control systems, the discrete equivalents to analog models are traditionally designed to process sequences of input and output samples such that each new output value accurately reproduces the corresponding analog output at the current sampling time. This paper addresses the fact that the performance of the resulting discrete equivalents is decreased by the inherent phase delay of analog models that alters the correlation between input and output sequences. Accordingly, a minimax procedure is proposed to reduce the digitizing error by shifting the entire output sequence with respect to the input sampling times. Then, a previously proposed interpolation based digitizing method is used to provide (i) a synchronous output, or (ii) an output that compensates for both the latency in computing the control law and the delay due to the zero-order hold in the D/A converter, or (iii) a state-space design with a hybrid controller that eliminates the zero-order hold altogether.**

I. INTRODUCTION

Numerous efforts have been directed in the field of digital signal processing toward the optimal design of infinite impulse response (IIR) digital filters that approximate prescribed magnitude and phase responses [1], [2]. This type of frequency-domain design was also applied to the problem of creating discrete equivalents to continuous transfer functions with better results than the early methods that were primarily meant for hand computations. Next, a time-domain method – referred to as the extended window design (EWD) of IIR filters [3] – was shown to be equivalent to the traditional weighted least squares (WLS) filter design with frequency sampling [4] by using the so-called matched-pole (MP) frequency sampling design [5]. Yet, both the conventional and optimal digitizing methods encountered in the design of digital control systems suffer from limitations due to the restrictive nature of the discrete representation of continuous systems. Specifically, the finite input and output sequences that are related through discrete equations strictly correspond to the sampled values of their continuous counterparts regardless of the fact that the continuous output incorporates a phase delay. This delay of the continuous model affects the accuracy of the current input and output components of the discrete equations in the following ways: (i) the input along the last few sampling periods has little effect on the current output sample, (ii) the output samples depend on input samples that occurred prior to the input samples in the current equation, and (iii) the input and output sequences are not well correlated at sampling times.

The major contribution of this paper is twofold. First, a fast algorithm is proposed to minimize the digitizing error by generating the output sequence at equally spaced time instants corresponding to a *fractional* time shift with respect to the input sequence. This is the main input/output relationship whose accuracy reduces the round-off error propagation during the recursive computation of the output. Also, a versatile numerical representation of the prediction interval that covers one sampling period beyond the current sampling time is derived. Second, a few options become available in control system applications which require either a current output sample at the current sampling time, or an output that extends over the prediction interval. The latter is highly desirable in order to avoid the problems related to the latency in computing the control law and the delay due to the hold element of the D/A converter.

The paper is organized as follows. Section II formulates the control system problem and offers a unified description of the above mentioned mathematical tools – the EWD and MP methods. Then, the original EWD and MP equations are modified in the spirit of the proposed optimization method. It is shown that both the basic discrete equations and the prediction fundamentally differ from a previously proposed prediction method [6]. Section III deals with the practical aspects of the real-time implementation in digital control systems exemplified on the design of a regulator system with state estimator and integral control. The main conclusions are summarized in Section IV.

II. PROPOSED OPTIMIZATION METHOD

The problem of computing accurate discrete equivalents to continuous models is encountered in many digital control applications. In contrast to the design of frequency-selective digital filters, where additional delays up to a few sampling periods are usually accepted, the digital control design should not increase existing delays, rather exhibit some prediction features. At the same time, the control system components and signals are characterized by low bandwidth relatively to the folding frequency π/T, where T is the sampling period. Accordingly, the signal processing involved in the design of the discrete equivalents can be efficiently done with interpolation methods [7], in conjunction with a moderate extrapolation based on the dimensionality theorem [8]. The latter allows for an accurate extension of the signal approximation interval that will be used in the final implementation of the proposed digitizing method.

Manuscript received March 8, 2006.

The author is with the Electrical and Computer Engineering Department, Gonzaga University, Spokane, WA 99258, USA (phone: 509-323-3536, fax: 509-323-5871, e-mail: braileanu@gonzaga.edu)

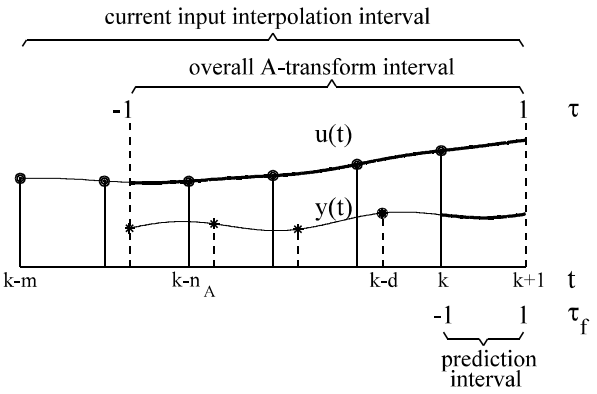

Fig. 1. Interpolation intervals for m=5, n_A=3, and d=0.7. Definitions of some normalized variables according to Section II-A below: t = the time normalized to the sampling period; τ = the A-transform time variable used over the interval $k\text{-}n_A\text{-}d \le t \le k+1$ in the design of the *main recursive equation*; τ_f = the A-transform variable of the fractional prediction interval $k \le t \le k+1$.

In the following, the continuous system to be digitized is defined in terms of a transfer function $H(s)$ obtained either directly from some physical equations or from a reduced-order state space model. The input and output signals are, respectively, denoted by $u(t)$ and $y(t)$, without associating them at this time with any particular control system signals. Thus, $u(t)$ may represent the input reference signal in a model following system, or the control signal itself in a plant model, or even the system output – usually denoted by $y(t)$ – like in the regulator example in Section III below, where $H(s)$ represents the *collapsed* integrator and state estimator.

The EWD and MP filters defined, respectively, in [3] and [5], are digital equivalents of a continuous model with the transfer function

$$H(s) = \frac{Y(s)}{U(s)} = \frac{N(s)}{D(s)}, \qquad (1)$$

where $N(s)$ and $D(s)$ are known polynomials of orders m_A and n_A, respectively. Without loss of generality, the time is assumed to be normalized to the sampling period T of the input signal, and so the *folding frequency* will be $\omega_f = \pi$. The EWD filters are the result of a *joint time-frequency method* which is based on the interpolation of the input signal $u(t)$ at equally spaced sampling time as shown in Fig. 1 above. In addition to targeting the time domain $[k\text{-}m,k+1]$, the EWD interpolation targets a frequency domain $\omega \in [\omega_0,\omega_M] \subset [0,\pi]$ by expressing the input signal in terms of the trigonometric polynomial

$$u(t) = \sum_{n=0}^{M} (\alpha_n \cos \omega_n t + \beta_n \sin \omega_n t), \quad k-m \le t \le k, \qquad (2)$$

where $\omega_0, \ldots, \omega_M$ are distinct *frequency knots* of the interpolation problem. The frequency knots are usually chosen to be equally spaced within the frequency range $[\omega_0,\omega_M]$ that contains most of the spectral energy of $H(j\omega)$. Also, in the basic EWD method, M and m are chosen such that the coefficients α_n and β_n are obtained as the *exact solution* of the algebraic equations

$$\sum_{n=0}^{M} (\alpha_n \cos \omega_n t_k + \beta_n \sin \omega_n t_k) = u(t_k), \qquad (3)$$

where $u(t_k)$ are the values of the input signal at the sampling times t_k=k-m ,..., k. Then, the response $y(t)$ to the approximation $u(t)$ in (2) is to be determined and sampled to provide the output of the discrete equivalent to $H(s)$. Yet, the details related to initial conditions and output sampling are essential in the ensuing method.

The optimization steps that are proposed in this paper address the three problems (i)-(iii) mentioned in Section I, and can be described on Fig. 1. First, the interpolation interval is extended to the left in order to add past input samples to the expression of $u(t)$ in (2) and, consequently, to the equation that will produce the output samples. At the same time, the well-known fact that the error of the interpolation at equally spaced points is significantly higher within the end segments of the interpolation interval (see, e.g., [7]) is taken into account by removing part of the left end from the segment of $u(t)$ that is used in the computation of the response $y(t)$. Nevertheless, the inherent delay of $H(s)$, together with the above mentioned dimensionality theorem, allows for an extension of the approximation interval to the right of the current sampling time k, up to $(k+1)$. This amounts to an increase of m, while keeping n_A unchanged. Finally, the most effective increase of the digitizing accuracy will be obtained by applying a *fractional* time shift d to the output sequence with respect to the actual sampling times; both delays (d>0) and advances (d<0) are considered.

A. Numerical Generation of the Main EWD Matrix Invariants

In order to provide some output prediction, while the accuracy of the main recursive equation of the discrete equivalent is obtained with a predetermined fractional time shift, the proposed design uses continuous approximations of $u(t)$ and $y(t)$. These approximations cover the interval $t \in [k\text{-}n_A\text{-}d,k+1]$ and are expressed in terms of vectors of Chebyshev series coefficients. For convenience, the mapping of square integrable functions into the space of square summable vectors defined over the field of real numbers was referred to in [3] as the *A-transformation*. Basically, the *A-transform* $\mathbf{y}$ of a signal $y(t)$, $t \in [T_1, T_2]$, is the vector $\mathbf{y} = Ay(t)$, whose components are the coefficients of the Chebyshev series expansion of $y(t)$. The *inverse A-transform* is defined by

$$y(t) = [0.5, c_1(\tau), c_2(\tau), \ldots]\,\mathbf{y}, \quad \tau = \frac{2t-(T_2+T_1)}{T_2-T_1}, \qquad (4)$$

where $c_n(\tau) = \cos(n \arccos \tau)$ are the Chebyshev polynomials of the first kind, and τ is a normalized time variable. It is worth noting that, for any given τ and length N_y of $\mathbf{y}$, the explicit computation of the values $c_n(\tau)$ can be avoided, such that *only N_y multiplications are required*. Assume now that $\mathbf{y}$ is the *A*-transform of the output signal $y(t)$ of $H(s)$, defined in Fig. 1 on the interval $k\text{-}n_A\text{-}d \le t \le k+1$, corresponding to $-1 \le \tau \le 1$. Then, this vector, restricted to the first N_c coefficients may be used to generate the vector $\mathbf{y}_0$ of the interpolated output,

$$\mathbf{y}_o = \mathbf{P}_o\,\mathbf{y}, \quad \mathbf{P}_o: N_o \times N_c, \qquad (5)$$

calculated at any given times $t_o = \{t_i\}_{i=1,2,\ldots,No}$, $t \in [k\text{-}n_A\text{-}d,k+1]$. The i^{th} row of the matrix P_o is $[0.5, c_1(\tau_i), c_2(\tau_i),\ldots]$ and is

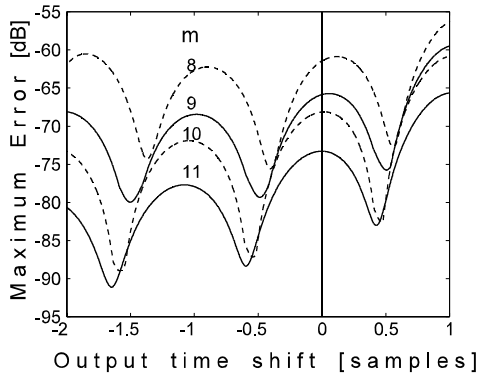

Fig. 2. Typical optimization diagram: distribution of the digitizing error for fixed n_A (n_A=8), a delay range $0 < d < 2$, and a prediction range $-1 < d < 0$.

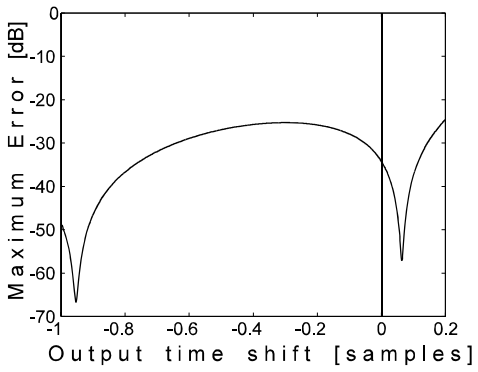

Fig. 3. Optimization diagram for the digitizing of the compensator (1") with transfer function $H(s)$: distribution of the digitizing error for n_A=7, m=9, a delay range $0<d<1$, and a prediction range $-0.2 <d< 0$.

calculated with (4), where $T_1=k-n_A-d$, $T_2=k+1$, τ_i corresponds to t_i, and $-1\le \tau_i \le 1$.

With this technique, the auxiliary conditions required by the computation of the response $y(t)$ can be introduced in the form of a matrix P_d calculated with (5) for a particular set of time instants. Specifically, a time shift d may be chosen such that the digital filter output $y_D(k)$, calculated at the current time $t=k$, actually represents the analog output corresponding to the time instant $t=k-d$. The EWD recursive generation of the current output $y(k-d)$ in Fig. 1 is based on the A-transform of the response $y(t)$, $k-n_A-d\le t\le k+1$, of the analog prototype $H(s)$ to the interpolated signal $u(t)$ built from the last $(m+1)$ input samples up to the time $t=k$. Moreover, $y(t)$ is determined along the time segment, $k-n_A-d\le t\le k+1$, while the auxiliary conditions are the last n_A output samples, $y(k-n_A-d), \ldots, y(k-d-1)$. Thus, this design, referred to as the *extended window design* (EWD) provides a natural match for the auxiliary conditions of the analog and digital filters and incorporates the interpolation step into the s- to z-domain mapping step. The "current sets" of input and output samples used as *auxiliary conditions* during the computation of the analog filter response are grouped into the vectors $\mathbf{u}_{aux}$ and $\mathbf{y}_{aux}$:

$$\begin{cases} \mathbf{u}_{aux} \triangleq \left[u_k, u_{k-1}, \ldots, u_{k-m} \right]^T, \\ \mathbf{y}_{aux} \triangleq \left[y_{k-d-1}, y_{k-d-2}, \ldots, y_{k-d-n_A} \right]^T . \end{cases} \tag{6}$$

Now, (2) is used to compute the A-transform $\mathbf{u}$ of $u(t)$ on the subinterval $k-d-n_A\le t\le k+1$ of $k-m\le t\le k+1$ in terms of the vector $\mathbf{u}_{aux}$ defined in (6). Thus, the *A-transform interpolation operator* $C(m,n_A,d)$ is defined by the following matrix relation

$$\mathbf{u} = \mathbf{C}(m,n_A,d)\,\mathbf{u}_{aux} . \tag{7}$$

As the A-transform reduces the computation of the response of the analog filter $H(s)$ to a linear algebra problem, a first general expression for the A-transform $\mathbf{y} = Ay(t)$ is obtained through matrix inversion,

$$\mathbf{y} = -\mathbf{G}\,\mathbf{y}_{aux} + \mathbf{F}\,\mathbf{u}_{aux}. \tag{8}$$

The parameters G and F in (8) are calculated once and for all for any given transfer function $H(s)$. Then, the inverse A-transform (4) is to be applied to both sides of (8) in order to yield $y(t)$ at any desired time instant $k-n_A-d\le t\le k+1$. In particular, the choice $t=k-d$ provides the *main recursive equation*

$$y_k = -\mathbf{g}^T \mathbf{y}_{aux} + \mathbf{f}^T \mathbf{u}_{aux} . \tag{9}$$

Likewise, (4) and (8) will be used in Section III below to compute any predicted values within the interval $k \le t \le k+1$.

B. The Matched-Pole Frequency Sampling Design

While the above time-domain interpolation method provides the solution for the implementation of an output prediction, the derivation of the main recursive equation (9) requires an efficient search for the time shift d that minimizes the digitizing error. This task will be achieved with an algorithm originally proposed in [5] as a modified version of the conventional IIR frequency sampling design [4]. This algorithm, referred to as the *matched-pole* (*MP*) *frequency sampling design*, is outlined below in order to provide a form suitable for the general case of a fractional time shift d.

First, the EWD problem is reformulated as the discrete-domain approximation of the frequency response of a system whose transfer function is

$$H_1(s) = e^{-ds} H(s) , \tag{1'}$$

where $H(s)$ was defined in (1). This approximation of $H_1(s)$ by

$$H_D(z) = \frac{p_0 z^m + p_1 z^{m-1} + \ldots + p_m}{z^{m-n_A}\left(z^{n_A} + g_1 z^{n_A-1} + \ldots + g_{n_A}\right)} = \frac{N_D(z)}{D_D(z)} \tag{10}$$

is a problem of complex approximation that is solved by frequency-domain interpolation with the interpolation points placed on the unit circle. Since both $H_1(s)$ and $H_D(z)$ are analytical rational functions, the properties of analytic functions imply some rather powerful constraints on their behavior within their respective regions of convergence. The MP design uses a consequence of the constraints on the frequency responses $H_1(j\omega)$ and $H_D(e^{j\omega})$ that relates the poles of $H(s)$ and $H_D(z)$ through the expression $z_n = e^{s_n}$.

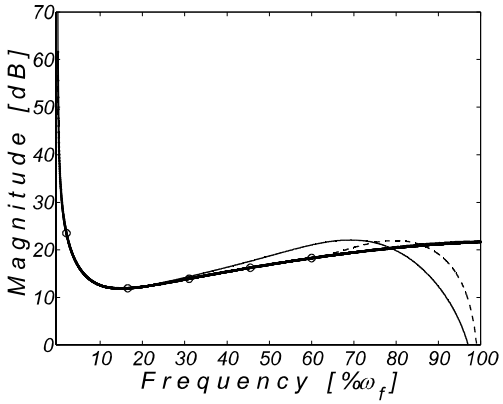

Fig. 4. Magnitude responses – *thick solid line*: $|H(j\omega)|$ and $|H_D(e^{j\omega})|$ of the optimal EWD compensator designed with d=0.953 and using the five frequency knots shown as *small circles* (the two plots practically coincide); *dashed line*: EWD compensator calculated with d = 0; *thin solid line*: compensator calculated with the bilinear transformation.

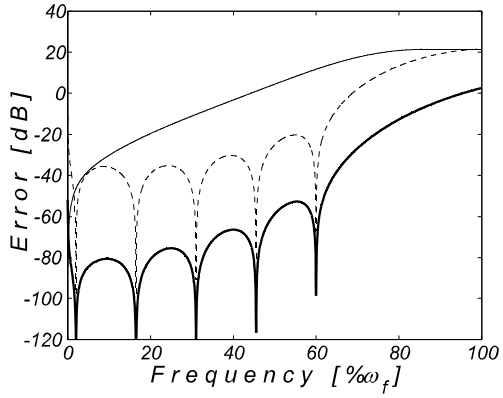

Fig. 5. Digitizing errors $E_D(\omega)$ of the three digital equivalents to the transfer function $H(s)$ shown in Fig 4 – *thick solid line*: the optimal EWD compensator $H_D(e^{j\omega})$ (n_A=7, m=9, d=0.953); *dashed line*: EWD compensator calculated with d = 0; *thin solid line*: compensator calculated with the bilinear transformation.

The proposed numerical design is based on this *pole-matching condition* and aims at matching the two frequency responses within a frequency range $[\omega_0,\omega_M]$ that contains most of the spectral energy of $H_1(j\omega)$. The set of algebraic equations

$$N_D(e^{j\omega_n}) = e^{-jd\omega_n} D_D(e^{j\omega_n}) H(j\omega_n), \quad n = 0, \ldots, M, \quad (11)$$

is solved for the (m+1) coefficients p_n defined in (10), while $D_D(z)$ is chosen with the same coefficients g_k, k=1, ..., n_A, as those found in the vector **g** in (9). Here, M and the *frequency knots* $\omega_0, \ldots, \omega_M$ are chosen in the same way as in (2), that is such that (11) has a unique solution. The time shift d makes the output $y_D(k)$, calculated at the current time t=k, actually represent the analog output at the time instant t=k-d.

Considering the above modified form of the MP design, the proof of its rigorous equivalence with the EWD method follows exactly the same lines as the proof given in [5] for the original forms of these two designs. Accordingly, the MP design determines precisely the same numerator coefficients p_n as found in the vector **f** in the EWD equation (9).

Finally, it is worth noting the close relationship between the EWD and MP filter design methods and the traditional WLS design [4]. The latter minimizes the expression

$$\min_{p_\ell, g_\ell} \sum_{n=0}^{M} w(\omega_n) \left| e^{-jd\omega_n} H(j\omega_n) - H_D(e^{j\omega_n}) \right|^2, \quad (12)$$

where p_ℓ and g_ℓ are the unknown coefficients of the numerator and denominator of $H_D(z)$, ω_n are the frequency knots within $[0,\pi]$, and $w(\omega)$ is a user defined weighting function. Yet, when approximating the transfer function of a continuous system by a discrete transfer function, the analyticity properties discussed above state that the denominator of $H_D(z)$ can be uniquely computed through the mapping $z_n = e^{s_n}$. Numerous tests have shown that the discrete equivalents to continuous transfer functions obtained with the EWD/MP approach yield about the same digitizing errors as the discrete equivalents provided by iterative WLS designs.

C. Minimization of the Digitizing Error

The proposed optimization deals only with the derivation (11) of the numerator coefficients p_n defined in (10), which are the same as those found in the vector **f** in (9). This computation is to be done repeatedly for values of the time shift d within an interval [-1,1]. At this time, there is no need for the complete EWD procedure that involves the interpolation (2) as well. Therefore, the above discussed equivalence between the EWD and MP methods and the simple form of (11) led to the MP-based search procedure that minimizes the digitizing error $E_D(\omega) = 20 \log_{10}(|e^{-jd\omega} H(j\omega) - H_D(e^{j\omega})|)$. A fast numerical algorithm was built by using the matrix form corresponding to the MP equation (11) and the fact that most of the components in (11) and $E_D(\omega)$ do not change as d changes. The algorithm was further improved by using to advantage the symmetry of the complex approximation dealing with rational functions with real coefficients.

A typical diagram displaying the distribution of the digitizing error $E_D(\omega)$ is shown in Fig. 2 for a given order, n_A, of the continuous transfer function $H(s)$ (n_A=8), a delay range $0 < d < 2$, and a prediction range $-1 < d < 0$. This diagram supports previous notifications about improved performance of the discrete transfer function by increasing the number of coefficients in the numerator (i.e., increasing m) while keeping n_A unchanged. This fact was mentioned in [1] and [2] without discussing the reasons why, and only a partial justification was presented in [3] and [5]. A more detailed justification was given above, at the end of the introductory part of this section. But the most important result is the error decrease found in the valleys in-between the input sampling times. *These valleys are deep enough to make a difference in either case, delay* or *advance*; also, they are not excessively narrow, thus allowing for the use of processors with reduced-word arithmetic. This result represents a substantial improvement with respect to the previously reported error decrease through integer delay [3], [5]. For example, this can be verified by checking the error values at abscissa points 0 and -1 in Fig.2.

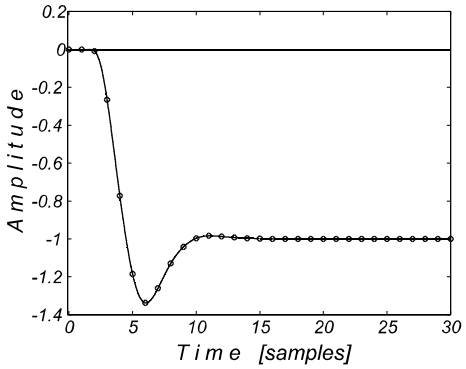

Fig. 6. Response $u(t)$ of the compensator (1") in the closed-loop system to a step disturbance applied to the plant input – *small circles*: discrete output of the optimal EWD compensator $H_D(e^{j\omega})$; *solid line*: response of the continuous model $H(s)$.

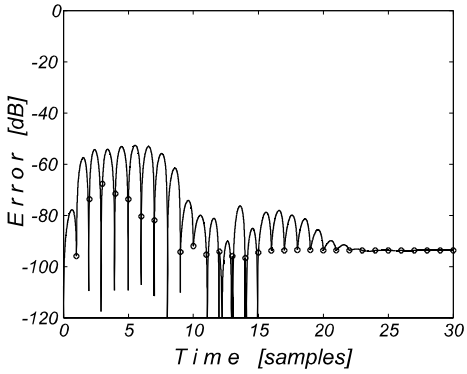

Fig. 7. Time-domain error of the response $u(t)$ of the optimal EWD compensator $H_D(e^{j\omega})$ shown in Fig. 6 – *small circles*: error at the sampling times; *solid line*: interpolation error with respect to the actual response of the continuous model $H(s)$.

Moreover, the minimum in the prediction interval brings an additional advantage with respect to the method proposed in [6] where no optimization was performed.

III. DESIGN EXAMPLE

The proposed optimal digitizing method and a few implementation options are illustrated on the design by emulation of a regulator with state estimator and integral control. The input-output transfer function of the plant $Y(s)/U(s) = H_a(s)H_b(s)$ is described by a wideband block with the transfer function

$$H_a(s) = \frac{16^7 (s+16)(s^2+s+16)}{(s^2+2s+16)(s^2+4s+16)(s^2+40s+1000)(s^2+20s+600)(s^2+2s+512)}$$

followed by a narrowband block with the transfer function

$$H_b(s) = \frac{0.5}{(s+1)(s+0.5)} .$$

A balanced model reduction [9] was applied to a state-space representation of the resulting transfer function $H_a(s)H_b(s)$ to provide the matrices A, B, C, and D (D = 0), corresponding to

$$H_r(s) = \frac{(s+10.59)(s^2-24.27s+226.59)(s^2+1.007s+15.99)}{341.6(s+1)(s+0.5)(s^2+2.01s+15.89)(s^2+4.062s+16.19)}$$

The regulator system with state estimator and integral control [10] is designed for constant reference input (r = 0).The following signals are defined: $u(t)$ – the control signal, $w(t)$ – a step disturbance, $y(t)$ – the output of the plant, $\mathbf{x}(t)$ – the state vector of the plant, $\mathbf{x}_o(t)$ – the state vector of the state estimator, and $x_i(t)$ – the output of the error integrator. The system is described by the following state equations

$$\begin{aligned} \dot{\mathbf{x}} &= \mathbf{A}\,\mathbf{x} + \mathbf{B}\,u + \mathbf{B}\,w \\ \dot{\mathbf{x}}_o &= (\mathbf{A} - \mathbf{L}\,\mathbf{C} - \mathbf{B}\,\mathbf{K})\,\mathbf{x}_o - \mathbf{B}\,\mathbf{K}_i\,x_i + \mathbf{L}\,y \\ \dot{x}_i &= -y \\ u &= -\mathbf{K}\,\mathbf{x}_o - \mathbf{K}_i\,x_i , \end{aligned} \qquad (13)$$

where the row-vector K, the scalar K_i, and the column-vector L were computed by slightly modifying the standard design [10] in order to ensure the stability of the compensator.

In (13), $y(t)$ is the input of the compensator, while its output is $u(t)$. Thus, both the EWD and the MP optimization design were applied to the following compensator transfer function

$$H(s) = \frac{U(s)}{Y(s)} = \frac{-83.76(s+23.28)(s+5.26)(s^2+6.228s+18.14)(s^2+1.81s+0.843)}{s(s^2+11.4s+45.45)(s^2+12s+45)(s^2+11.4s+41.49)} . \qquad (1")$$

First, the MP optimization described in Section II-C was done on (1") with a sampling period T = 0.5 and a length of the input interpolation interval m = 9. Thus, a time normalization to the sampling period T was performed and the minimax procedure was applied for a wide range of the normalized time shift parameter d. Each point of the resulting diagram in Fig. 3 was obtained by solving a pre-processed form of (11) as described in Section II-C and calculating the maximum of the digitizing error $E_D(\omega) = 20\log_{10}(|e^{-jd\omega}H(j\omega)-H_D(e^{j\omega})|)$ within a frequency interval $\omega_0<\omega<0.6\ \omega_f$ (where ω_0 is the first frequency knot and $\omega_f = \pi/T$ is the folding frequency). Fig. 3 is restricted to the delay range $0 < d < 1$ and the prediction range $-0.2<d<0$, and exhibits the two optimum time shifts corresponding to a delay d = 0.953 and a prediction d=-0.065. The discrete model (10) designed with d =-0.065 has the transfer function $H_D(z)$ with a factor -7.5597, numerator zeros at 0.299443, -0.339056 ± j 0.324061, 0.022866 ± j 0.39033, 0.635847 ± j 0.051755, 0.245423 ± j 0.237634, and seven poles defined by the expression $z_n = e^{s_n T}$, n=1,2,...,7, where T=0.5 and s_n are the poles of $H(s)$ in (1") . The remaining two poles are placed at z = 0.

The frequency response of the compensator defined in (1") is compared in Fig. 4 to the frequency responses of a few discrete realizations. It is worth mentioning that the magnitude plot $|H_D(e^{j\omega})|$ of the optimal EWD compensator corresponding to the minimum shown in Fig. 3 practically coincides with the plot $|H(j\omega)|$ of the continuous model. By contrast, the sensibly larger digitizing errors of other designs are apparent even on the magnitude plots. This is the case with both the EWD compensator calculated with d = 0 and the compensator calculated with the bilinear transformation. More details on the digitizing error $E_D(\omega)$ can be seen in Fig. 5.

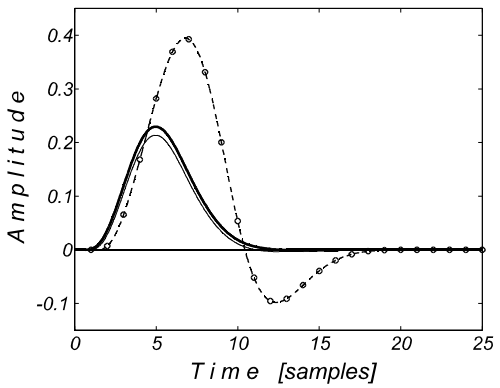

Fig. 8. Closed-loop system response $y(t)$ to a unit-step disturbance applied to the input of the plant – *thick solid line*: $y(t)$ for the continuous design with compensator (1"); *thin solid line*: $y(t)$ obtained with the discrete optimal EWD compensator $H_D(e^{j\omega})$; *dashed line with small circles*: $y(t)$ corresponding to the direct digital system design.

Another look at the performance of the optimal EWD compensator is done by using the closed-loop response $y(t)$ of the system (13) to a unit-step disturbance applied at the input of the plant. The signal $y(t)$ and its sampled sequence were applied, respectively, to $H(s)$ defined by (1") and the above $H_D(z)$. The comparison is done in Figs. 6 and 7. In Fig. 6, the small circles that represent the response of the EWD model $H_D(z)$ to $y(kT)$ practically coincide with the response of the continuous compensator $H(s)$. This is supported by the very small error exhibited by the small circles in Fig. 7. In addition, the solid line in Fig. 7 represents the interpolation error with respect to the actual response of the continuous model $H(s)$.

Finally, the above design of the discrete compensator with the optimal EWD method is compared in Fig. 8 with the direct digital system design [11]. Here, a simple application of the proposed method to the state-variable system design was considered. Specifically, two discrete equations were implemented: the main recursive equation

$$y_k = -\mathbf{g}^T \mathbf{y}_{aux} + \mathbf{f}^T \mathbf{u}_{aux} \qquad (9')$$

and

$$y_p = -\mathbf{g}_p{}^T \begin{bmatrix} y \\ \mathbf{y}_{aux} \end{bmatrix} + \mathbf{f}_p{}^T \mathbf{u}_{aux}, \qquad (14)$$

where the vectors $\mathbf{g}_p$ and $\mathbf{f}_p$ were obtained from the matrices G and F in (8), by applying the inverse A-transform (4) to $\mathbf{y}$ in a particular form of (8) restricted to the prediction interval shown in Fig. 1. Accordingly, the variable τ in (4) was replaced by τ_f in Fig. 1, whereas the vector $\mathbf{y}_{aux}$ was augmented with the last computed output sample y_k in (9'). The inverse A-transform was calculated at only one point $\tau_f = 0$, corresponding to the middle of the prediction interval. This prediction alleviates the effect of the zero-order hold in the D/A converter.

IV. CONCLUSION

The focus in this paper was on the proposed optimal digitizing procedure which provides the main recursive equation (9) and, optionally, either a second equation (14) that computes an output value corresponding to some future time, or a few coefficients of the Chebyshev polynomial expansion contained in the vector $\mathbf{y}$ in (8). The accuracy of (9) reduces the round-off error propagation during the recursive computation of the output samples. At the same time, (8) and (14) can be implemented with reduced-word arithmetic thus reducing the computational requirements.

This problem of computing accurate discrete equivalents to continuous models is encountered, for example, in the design of model following systems, controllers with prediction, or compensators with integrators and state estimation. The latter was used in Section III only in order to illustrate the fact that the high accuracy of the proposed method, together with its prediction feature, provides a fully satisfactory controller even in the presence of a zero-order hold. Moreover, the present technology allows for a relatively inexpensive implementation of the above mentioned polynomial expansion, say, with three coefficients, in the form of a hybrid controller involving both continuous-time and discrete-time signals. It is expected that this solution would provide a response close to that one of a continuous controller. Finally, future work will evaluate the performance of the above prediction design with zero-order hold, the hybrid controller design, and the sampled-data design methods that incorporate the intersample behavior but preserve the zero-order hold constraint on the control signal [12].

REFERENCES

[1] H. G. Martinez and T. W. Parks, "Design of recursive digital filters with optimum magnitude and attenuation poles on the unit circle," *IEEE Trans. ASSP*, vol.26, pp. 150-156, Apr. 1978.

[2] M.C. Lang,"Least-squares design of IIR filters with prescribed magnitude and phase responses and a pole radius constraint," *IEEE Trans. ASSP*, vol.48, pp. 3109-3121, Nov. 2000.

[3] G. I. Braileanu, "Extended-window interpolation applied to digital filter design," *IEEE Trans. Signal Processing*, vol. 44, pp. 457-472, March 1996.

[4] C. S. Burrus and T.W. Parks, *Digital Filter Design*, New York: Wiley, 1987.

[5] G. I. Braileanu, "Equivalence between the extended window design of IIR filters and least squares frequency domain designs," in *Proc. 2003 Int. Conf. on Acoustics, Speech, and Signal Processing* (*ICASSP* 2003), vol. VI, pp. 21-24, Hong Kong, 2003.

[6] G. I. Braileanu, "Digitizing method with application to the design of fractional-time prediction models," in *Proc.* 43*rd IEEE Conference on Decision and Control* (*CDC* 2004), Paradise Island, Bahamas, 2004, pp. 2340-2345.

[7] M. J. D. Powell, *Approximation Theory and Methods*, Cambridge, London: Cambridge Univ. Press, 1981.

[8] L. W. Couch II, *Digital and Analog Communication Systems*, New York: Macmillan, 1990, pp. 96-98.

[9] B. C. Moore, "Principal component analysis in linear systems: controllability, observability, and model reduction," *IEEE Trans. Automatic Control*, vol. 26, pp. 17-32, Jan. 1981.

[10] G. F. Franklin, J. D. Powell, and A. Emami-Naeini, *Feedback Control of Dynamic Systems*, Reading, MA: Addison Wesley, 1994, pp. 493-553.

[11] G. F. Franklin, J. D. Powell, and M. L. Workman, *Digital Control of Dynamic Systems*, Menlo Park, CA: Addison Wesley, 1998, pp. 280-327.

[12] T. Chen and B. Francis, *Optimal Sampled-Data Control Systems*, New York: Springer-Verlag, 1995.